Pharmaceutics, Drug Delivery and Pharmaceutical Technology

Assessing the Detection Limit of a Minority Solid-State Form of a Pharmaceutical by ^{1}H Double-Quantum Magic-Angle Spinning Nuclear Magnetic Resonance Spectroscopy

Keisuke Maruyoshi [1,2], Dinu Iuga [1], Abigail E. Watts [3], Colan E. Hughes [3], Kenneth D.M. Harris [3], Steven P. Brown [1,*]

[1] Department of Physics, University of Warwick, Coventry CV4 7AL, UK
[2] Analytical and Quality Evaluation Research Laboratories, Daiichi Sankyo Co. Ltd., 1-12-1, Shinomiya, Hiratsuka-shi, Kanagawa 254-0014, Japan
[3] School of Chemistry, Cardiff University, Park Place, Cardiff, Wales CF10 3AT, UK

ARTICLE INFO

ABSTRACT

The lower detection limit for 2 distinct crystalline phases by ^{1}H magic-angle spinning (MAS) solid-state nuclear magnetic resonance (NMR) is investigated for a minority amount of cimetidine (anhydrous polymorph A) in a physical mixture with the anhydrous HCl salt of cimetidine. Specifically, 2-dimensional ^{1}H double-quantum (DQ) MAS NMR spectra of polymorph A and the anhydrous HCl salt constitute fingerprints for the presence of each of these solid forms. For solid-state NMR data recorded at a ^{1}H Larmor frequency of 850 MHz and a MAS frequency of 30 kHz on ~10 mg of sample, it is shown that, by following the pair of cross-peaks at a ^{1}H DQ frequency of 7.4 + 11.6 = 19.0 ppm that are unique to polymorph A, the level of detection for polymorph A in a physical mixture with the anhydrous HCl salt is a concentration of 1% w/w.
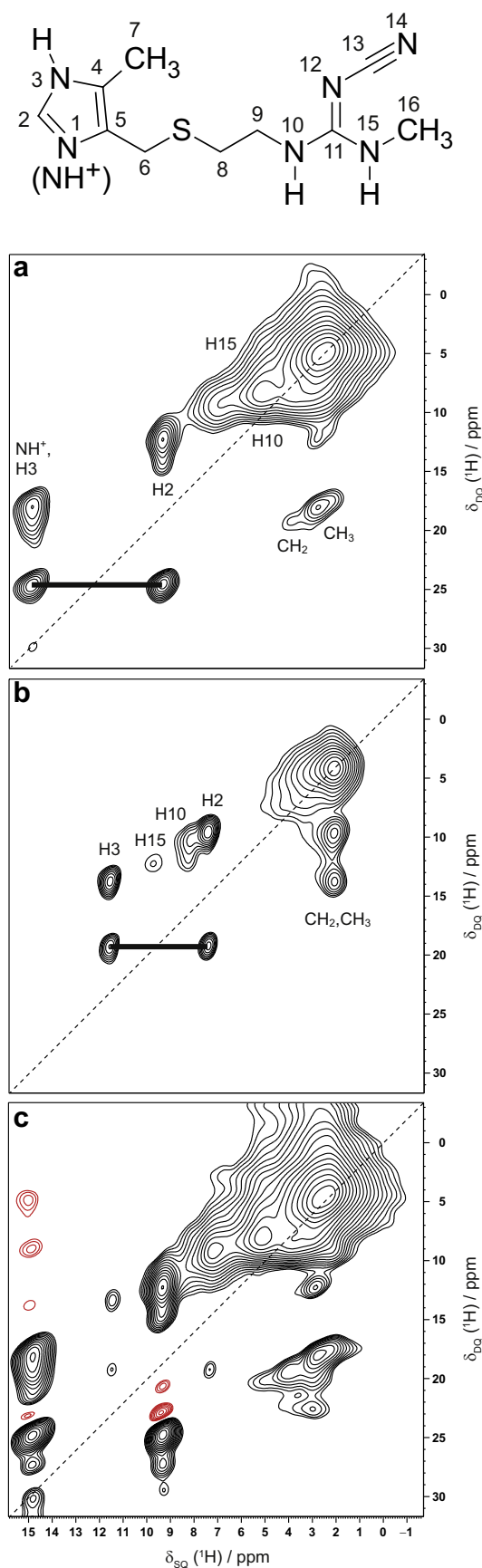
Introduction

Salt formation is the most general and effective method for improving the aqueous solubility and dissolution rate of acidic and basic drugs. Currently nearly half of all active pharmaceutical ingredients (APIs) used in medication are in salt forms.[1] However, during various processing steps such as milling, compression, drying, and granulation, a salt can become unstable chemically and physically, such that it may transform to its free acid/base form or into other polymorphs or solvates. Many of the commonly used excipients in tablet formulations are acidic or basic and can, thus, change the local pH of a system. This can affect the stability of the salt and cause the transformation of the salt to the corresponding free acid/base form. The solid-state transformation from a salt to a free form will alter key properties of the API, such as solubility and dissolution behavior, leading to undesired changes in the bioavailability of the API.[2] In order to monitor the quality of

pharmaceuticals, an effective and highly sensitive quantitation method is required.

A variety of techniques have been used to characterize the physicochemical properties of pharmaceuticals,[3] including powder X-ray diffraction (PXRD), differential scanning calorimetry (DSC), and vibrational spectroscopies, notably IR and Raman. Although PXRD is considered the definitive test for the identification of a specific solid-state form, the effectiveness of PXRD for quantitative analysis of mixtures of solid phases can be diminished when the effects of preferred orientation are significant[4]; however, if the crystal structures of all the solid forms present in the mixture are known, then quantitative analysis can be carried out by Rietveld refinement in which the effects of preferred orientation are taken rigorously into consideration. For example, Li et al.[5] have shown that the error associated with distinguishing polymorphs I and II of sulfamerazine by DSC or PXRD was ±3%, which is superior to that achieved by Raman spectroscopy. Siddiqui et al.[6] have also used PXRD (and solid-state nuclear magnetic resonance [NMR]) to quantify the amount of crystalline tacrolimus solid dispersions,[7] whereas Macfhionnghaile et al.[8] have investigated the effect of ball-milling and cryomilling on sulfamerazine using PXRD, IR, and near-IR spectroscopy. Using terahertz (THz) spectroscopy,[9]

* Correspondence to: Steven P. Brown (Telephone: 00 44 24 765 74359; Fax: 00 44 24 761 50897).
E-mail address: S.P.Brown@warwick.ac.uk (S.P. Brown).

Figure 1. ^{1}H (850 MHz) DQ MAS (30 kHz) spectra of (a) the anhydrous HCl salt of cimetidine, (b) polymorph A of cimetidine, and (c) a 10% w/w physical mixture of

Strachan et al.[10] have shown that the concentration of carbamazepine form III in a physical mixture with form I can be detected down to a concentration of 1.5%. Moreover, Hisazumi et al.[11] have used THz spectroscopy to distinguish between anhydrous and hydrate forms of theophylline with an error of 3% in a pharmaceutical formulation. Recently, Thakral et al.[12] have used PXRD to follow salt disproportionation, in which the PXRD data were measured using a 2-dimensional area detector—using this technique, conventional 1-dimensional PXRD patterns that are free from the effects of preferred orientation can be obtained by appropriate integration of the 2-dimensional data.

Solid-state NMR spectroscopy is an important method for pharmaceutical analysis.[13-17] Although the workhorse method is ^{13}C cross-polarization (CP) magic-angle spinning (MAS), the potential of applying ^{1}H fast MAS NMR is increasingly recognized for solid-state analysis.[18-48] In particular, the ^{1}H double-quantum (DQ) solid-state NMR experiment is a powerful probe of dipolar-coupled protons, with DQ peaks observed for close (typically less than 3.5 Å) through-space H⋅⋅⋅H proximities.[49-51] Thus, a 2-dimensional ^{1}H DQ spectrum represents a "fingerprint" for a specific 3-dimensional packing arrangement adopted by an organic molecule, emphasizing the advantage over 1-dimensional ^{1}H or ^{13}C NMR spectra of spreading out into 2 dimensions. In this way, by using a high-resolution ^{1}H DQ combined rotation and multiple-pulse spectroscopy (CRAMPS) approach,[52] it has been shown how the presence of only the anhydrous form and not a hydrate form of an API in tablet formulation can be established.[19] However, due to the spectral noise associated with the application of ^{1}H homonuclear decoupling in the CRAMPS approach, it is only possible to conclude that the hydrate form is absent within a detection limit of ~5% for the spectra presented in the study by Griffin et al.[19] An alternative approach is to use a combination of fast MAS and high magnetic field to give ^{1}H DQ MAS spectra, where the resolution, although not as good as with the ^{1}H DQ CRAMPS method,[51] is sufficient to resolve distinct spectral features. For the specific case of the anhydrous HCl salt of cimetidine (the crystal structure of which has been determined recently[53] by a combined PXRD and NMR crystallography strategy) and the free form of cimetidine (anhydrous polymorph A), this article investigates the lower limit of detection of a minority solid-state form of an API, present in a physical mixture with another crystalline phase of the same API, using ^{1}H DQ MAS NMR spectroscopy.

Experimental Section

Cimetidine and cimetidine hydrochloride were purchased from Sigma-Aldrich and used without further purification. The identification of the specific solid-state form was confirmed by PXRD as shown in the studies by Tatton et al.[33] and Watts et al.[53] Samples containing 10%, 5%, 1%, and 0.5% w/w polymorph A/anhydrous HCl salt were prepared by physically mixing appropriately weighed quantities of the 2 pure solid phases.

Solid-state NMR experiments were performed on a Bruker Avance III spectrometer operating at a ^{1}H Larmor frequency of 850.2 MHz (B_0 = 20.0 T) using a Bruker triple-resonance probe, operating

polymorph A and the anhydrous HCl salt. An assignment of the ^{1}H chemical shifts is presented in Table 1, while Tables 2 and 3 list the expected ^{1}H DQ peaks based on H⋅⋅⋅H proximities extracted from the geometry-optimized (CASTEP) crystal structures. The thick horizontal lines in (a) and (b) denote the pair of ^{1}H DQ peaks corresponding to the intramolecular proximity of the imidazole H2 (CH) and H3 (NH) protons, noting that for the anhydrous HCl salt this overlaps with the pair of ^{1}H DQ peaks corresponding to the intramolecular proximity of the imidazole H2 (CH) and H1 (NH$^+$) protons. The base contour levels are at (a) 5.4%, (b) 11%, and (c) 2.6% with respect to the maximum peak height. (Note that a conference abstract has presented the spectra in this figure in a different format.[72])

in double-resonance mode, supporting rotors of 2.5 mm outer diameter (corresponding to ~10 mg of sample). An MAS frequency of 30 kHz was used. The pulse sequence and coherence transfer pathway diagram for the ^{1}H DQ MAS[49] experiment using back-to-back recoupling[54,55] are shown in Figure 7 of the review by Brown and Spiess.[56] A 16-step phase cycle was used to select $\Delta p = \pm 2$ on the DQ excitation block and $\Delta p = -1$ on the final 90° pulse, where p is the coherence order. The ^{1}H 90° pulse duration was 2.5 μs. In all experiments, 160 t_1 FIDs were recorded with a rotor-synchronized t_1 increment of 33.3 μs using the States time-proportional phase incrementation method to achieve sign discrimination in F_1. For the anhydrous HCl salt of cimetidine and polymorph A of cimetidine, 16 transients were co-added with a recycle delay of 3 s. For the physical mixtures of polymorph A and the anhydrous HCl salt, a recycle delay of 9 s was used and 16 (10% and 5% w/w mixture samples), 48 (1% w/w mixture sample), and 112 (0.5% w/w mixture sample) transients were co-added. The experimental times were thus 2 h (anhydrous cimetidine hydrochloride and cimetidine polymorph A), 6 h (10% and 5% w/w mixture samples), 19 h (1% w/w mixture sample), and 44 h (0.5% w/w mixture sample).

^{1}H chemical shifts are referenced with respect to neat TMS using adamantane as a secondary reference (1.85 ppm for ^{1}H).[57] Experimental ^{1}H chemical shifts are stated to an accuracy of ±0.1 ppm.

Results and Discussion

^{1}H DQ MAS Solid-State NMR Spectra

In previous studies, 1-dimensional ^{13}C CP MAS NMR spectra, as well as the results of various heteronuclear dipolar experiments, have been presented for a free form of cimetidine (polymorph A),[58,59] whereas a ^{13}C CP MAS spectrum of the anhydrous HCl salt of cimetidine as well as a gauge-including projector-augmented wave (GIPAW) calculation[60,61] of the NMR parameters (for the reported crystal structure following geometry optimization) have been presented recently.[53] Tatton et al.[33] have also presented ^{15}N-^{1}H spectral-editing and ^{14}N-^{1}H and ^{15}N-^{1}H correlation spectra for polymorph A of cimetidine, together with GIPAW calculations of the chemical shielding and electric field gradient tensors for the reported crystal structure[62] following geometry optimization. Note that distances stated in this paper are from the geometry-optimized crystal structures on which these GIPAW calculations were carried out (available as Supporting Information in studies by Tatton et al.[33] and Watts et al.[53]).

Figures 1a and 1b present ^{1}H DQ MAS NMR spectra of (a) the anhydrous HCl salt of cimetidine and (b) polymorph A of cimetidine, recorded at a ^{1}H Larmor frequency of 850 MHz and an MAS frequency of 30 kHz. Because ^{1}H linewidths for the strongly dipolar-coupled network of protons in organic solids decrease with increasing MAS frequency,[63,64] narrower ^{1}H linewidths would be observed using the higher MAS frequencies of >60 kHz that can be achieved with rotors of smaller outer diameter (1.3 mm and less). However, the improved resolution would come at the cost of lower sensitivity associated with the considerably reduced sample volume (corresponding to sample mass ~1 mg or less). Enhanced resolution could also be achieved using the ^{1}H DQ CRAMPS approach (e.g., see Fig. 3 of the review by Brown[51]) but, as noted in the Introduction, the disadvantage of using ^{1}H homonuclear decoupling is the observation of additional "noise" in the spectra which limits the lower detection of the minority phase to ~5%. For these reasons, it was decided that 30-kHz MAS at a ^{1}H Larmor frequency of 850 MHz provided the best compromise of sufficiently high-resolution and optimum sensitivity for ^{1}H DQ MAS NMR spectroscopy of the anhydrous HCl salt and polymorph A of cimetidine—see the spectra presented in Figures 1a and 1b.

Table 1
Experimental[a] and GIPAW-Calculated[b] ^{1}H Chemical Shifts (in ppm) for the Anhydrous HCl Salt and Polymorph A of Cimetidine

Atom Label	Atom Descriptor	Anhydrous HCl Salt		Polymorph A	
		Experimental	Calculated	Experimental	Calculated
H1	NH$^+$	15.0	15.5	–	–
H2	CH	9.4	9.2	7.4	7.1
H3	NH	15.0	15.3	11.6	11.9
H6a	CH$_2$	3.6	4.3	4.0	3.4
H6b	CH$_2$	3.6	3.8	4.0	3.0
H7a-c[c]	CH$_3$	2.6	2.9	2.0	1.3
H8a	CH$_2$	2.6	2.4	3.0	1.3
H8b	CH$_2$	2.6	0.7	3.0	0.2
H9a	CH$_2$	2.6	2.8	3.0	2.4
H9b	CH$_2$	2.6	1.9	3.0	2.7
H10	NH	5.0	4.6	8.2	8.2
H15	NH	6.7	6.9	9.7	9.6
H16a-c[c]	CH$_3$	2.6	1.4	2.0	1.5

[a] It is not possible to distinguish some separate CH$_2$ and CH$_3$ ^{1}H resonances in the experimental spectra.
[b] Calculated isotropic chemical shifts are obtained from the calculated absolute shielding as $\delta_{iso}^{calc} = \sigma_{ref} - \sigma_{cal}$, where $\sigma_{ref} = 30.0$ ppm.
[c] For CH$_3$ groups, the stated value of the calculated isotropic chemical shift is the average for the 3 protons.

The ^{1}H DQ MAS NMR spectra presented in Figure 1 were recorded using 1 rotor period of back-to-back recoupling.[54,55] Such ^{1}H DQ MAS NMR spectra probe DQ coherences between pairs of through-space dipolar coupled protons corresponding to a close (typically less than 3.5 Å) H···H distance,[49,51] with DQ peaks

Table 2
H···H Proximities[a] (<3.5 Å) and Corresponding ^{1}H DQ Shifts (See Fig. 1a) for the NH and Imidazole CH Protons in the Anhydrous HCl Salt of Cimetidine

Atom Descriptor	Atom Label	δ_{SQ}/ppm	δ_{DQ}/ppm	Distance/Å
H1 (NH$^+$) (15.0 ppm)	H2 (CH)	9.4	24.4	2.57
	H6b (CH$_2$)	3.6	18.6	2.70
	H7c (CH$_3$)	2.6	17.6	2.82
	H16c (CH$_3$)	2.6	17.6	2.94
	H16a (CH$_3$)	*2.6*	*17.6*	*3.18*
	H3 (NH)	*15.0*	*30.0*	*3.43*
	H7a (CH$_3$)	2.6	17.6	3.49
H2 (CH) (9.4 ppm)	H1 (NH$^+$)	15.0	24.4	2.57
	H3 (CH)	15.0	24.4	2.57
	H7c (CH$_3$)	2.6	12.0	2.69
	H6b (CH$_2$)	3.6	13.0	2.82
	H6a (CH$_2$)	3.6	13.0	3.06
	H6a (CH$_2$)	3.6	13.0	3.13
	H16b (CH$_3$)	2.6	12.0	3.39
H3 (NH) (15.0 ppm)	H2 (CH)	9.4	24.4	2.57
	H6b (CH$_2$)	3.6	18.6	2.71
	H7c (CH$_3$)	2.6	17.6	2.73
	H6a (CH$_2$)	3.6	18.6	2.95
	H7b (CH3)	2.6	17.6	3.04
	H9a (CH$_2$)	2.6	17.6	3.15
	H16c (CH$_3$)	2.6	17.6	3.35
	H6a (CH$_2$)	3.6	18.6	3.39
	H1 (NH$^+$)	*15.0*	*30.0*	*3.43*
H10 (NH) (5.0 ppm)	H9a (CH$_2$)	2.6	7.6	2.29
	H9b (CH$_2$)	2.6	7.6	2.94
	H8b (CH$_2$)	2.6	7.6	2.98
	H7b (CH$_3$)	2.6	7.6	3.03
	H16c (CH$_3$)	2.6	7.6	3.31
	H8a (CH$_2$)	2.6	7.6	3.33
	H7a (CH$_3$)	2.6	7.6	3.36
H15 (NH) (6.7 ppm)	H9b (CH$_2$)	2.6	9.3	2.17
	H16a (CH$_3$)	2.6	9.3	2.24
	H8a (CH$_2$)	2.6	9.3	2.26
	H16b (CH$_3$)	2.6	9.3	2.72
	H16c (CH$_3$)	2.6	9.3	2.93
	H8a (CH$_2$)	*2.6*	*9.3*	*2.94*

Intermolecular proximities are in italics.
[a] Distances are stated for the geometry-optimized (CASTEP) crystal structure.

observed at the sum of the 2 single-quantum (SQ) frequencies. Table 1 presents an assignment of the experimentally observed ^{1}H chemical shifts for polymorph A and the anhydrous HCl salt of cimetidine based on GIPAW calculations (as reported previously).[33,53] The significant change in the ^{1}H chemical shift of H3 reflects the change from an NH···N intermolecular hydrogen bond with N12 as the acceptor in polymorph A (involving uncharged donor and acceptor groups) to an NH$^+$···Cl$^-$ intermolecular hydrogen bond (involving charged donor and acceptor groups) in the anhydrous HCl salt.

Tables 2 and 3 list H···H proximities under 3.5 Å for the NH and imidazole CH protons and the corresponding ^{1}H DQ shifts for the anhydrous HCl salt and polymorph A of cimetidine, respectively. For the anhydrous HCl salt, the NH$^+$ (H1) and NH (H3) imidazole ^{1}H chemical shifts overlap (at 15.0 ppm, see Table 1). Thus, in the ^{1}H DQ MAS spectrum in Figure 1a, the pair of ^{1}H DQ peaks at $\delta_{DQ} = 15.0 + 9.4 = 24.4$ ppm corresponds to an intramolecular proximity of 2.57 Å for the imidazole CH (H2) with both the NH$^+$ (H1) and NH (H3) protons—see Table 2. We also note the very weak diagonal peak at $\delta_{DQ} = 15.0 + 15.0 = 30.0$ ppm in Figure 1a that corresponds to a 3.43 Å intermolecular proximity of the NH$^+$ (H1) and NH (H3) protons (also see Table 2). As described in the study by Bradley et al.,[65] to a first approximation, the relative intensity of distinct ^{1}H DQ peaks at the same ^{1}H single-quantum chemical shift is proportional to the ratio of the square of the dipolar coupling constants and hence is inversely proportional to ratio of H···H distances to the sixth power—note that $(3.43/2.57)^6 = 5.7$. Other cross-peaks observed for the NH groups in the ^{1}H DQ MAS spectra in Figures 1a and 1b are due to intra- and intermolecular proximities to CH$_2$ and CH$_3$ protons (see Tables 2 and 3).

This study is focused on the pair of ^{1}H DQ peaks due to the intramolecular proximity of 2.57 and 2.55 Å for the imidazole H2

(CH) and H3 (NH) protons, whereby $\delta_{DQ} = 15.0 + 9.4 = 24.4$ ppm in Figure 1a for the anhydrous HCl salt and $\delta_{DQ} = 11.6 + 7.4 = 19.0$ ppm in Figure 1b for polymorph A. The evident change in the positions of the pair of ^{1}H DQ peaks due to the intramolecular proximity of the imidazole H2 (CH) and H3 (NH) protons between the anhydrous HCl salt and polymorph A constitutes a "fingerprint" that is a diagnostic for the presence of either or both of the distinct solid-state forms.

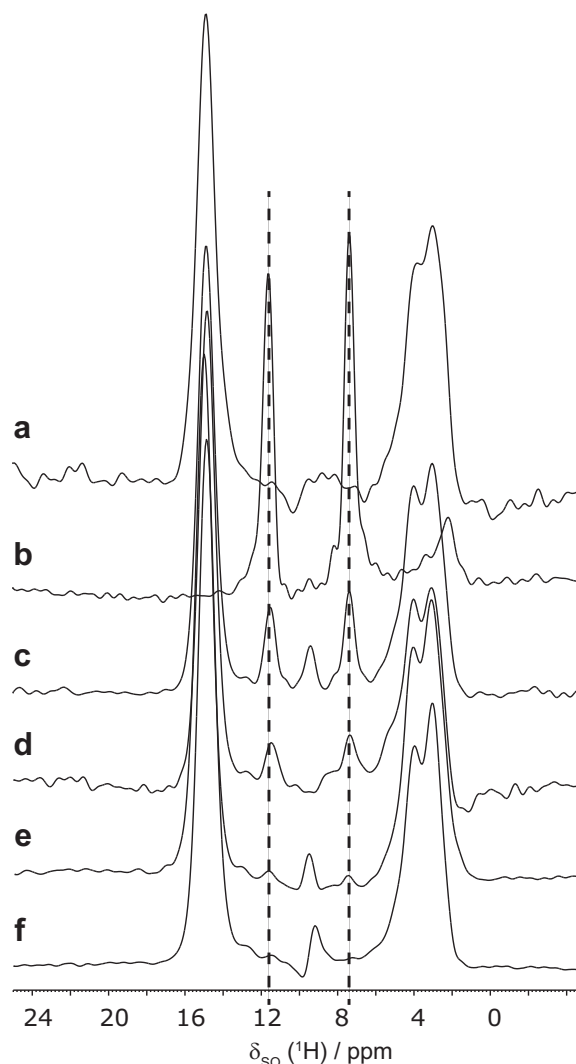### Probing the Level of Detection of a Minority Phase in a Physical Mixture of 2 Distinct Crystalline Phases

To determine the level of detection by ^{1}H DQ MAS NMR of polymorph A of cimetidine in a physical mixture with the anhydrous HCl salt of cimetidine, spectra were recorded for samples comprising 10%, 5%, 1%, and 0.5% w/w mixtures of polymorph A/anhydrous HCl salt. Specifically, Figure 1c presents a ^{1}H DQ MAS NMR spectrum of the 10% w/w mixture (note the lower base contour in Fig. 1c as compared to Figs. 1a and 1b). It is evident that a weak pair of ^{1}H DQ peaks at $\delta_{DQ} = 11.6 + 7.4 = 19.0$ ppm due to

Table 3
H···H Proximities[a] (<3.5 Å) and Corresponding ^{1}H DQ Shifts (See Fig. 1b) for the NH and Imidazole CH Protons in the Geometry-Optimized (CASTEP) Crystal Structure of Polymorph A of Cimetidine

Atom Descriptor	Atom Label	δ_{SQ}/ppm	δ_{DQ}/ppm	Distance/Å
H2 (CH) (7.4 ppm)	H3 (NH)	11.6	19.0	2.55
	H16a (CH$_3$)	*2.0*	*9.4*	*2.59*
	H7c (CH$_3$)	*2.0*	*9.4*	*2.87*
	H7a (CH$_3$)	*2.0*	*9.4*	*2.93*
	H15 (NH)	9.7	17.1	3.00
	H7b (CH$_3$)	*2.0*	*9.4*	*3.05*
	H6b (CH$_2$)	*4.0*	*11.4*	*3.27*
	H16c (CH$_3$)	*2.0*	*9.4*	*3.50*
H3 (NH) (11.6 ppm)	H16b (CH$_3$)	*2.0*	*13.6*	*2.52*
	H2 (CH)	7.4	19.0	2.55
	H7a (CH$_3$)	*2.0*	*13.6*	*2.59*
	H7b (CH$_3$)	*2.0*	*13.6*	*2.81*
	H7c (CH$_3$)	*2.0*	*13.6*	*3.09*
	H7b (CH$_3$)	*2.0*	*13.6*	*3.10*
	H16a (CH$_3$)	*2.0*	*13.6*	*3.13*
H10 (NH) (8.2 ppm)	H9a (CH$_2$)	3.0	11.2	2.27
	H16c (CH$_3$)	*2.0*	*10.2*	*2.71*
	H9b (CH$_2$)	3.0	11.2	2.93
	H8b (CH$_2$)	3.0	11.2	2.99
	H8a (CH$_2$)	3.0	11.2	3.42
H15 (NH) (9.7 ppm)	H9b (CH$_2$)	3.0	12.7	2.20
	H16a (CH$_3$)	*2.0*	*11.7*	*2.22*
	H8a (CH$_2$)	3.0	12.7	2.29
	H16c (CH$_3$)	*2.0*	*11.7*	*2.81*
	H16b (CH$_3$)	*2.0*	*11.7*	*2.90*
	H2 (CH)	7.4	16.1	3.00
	H6a (CH$_2$)	*4.0*	*13.7*	*3.19*
	H7b (CH$_3$)	*2.0*	*11.7*	*3.22*
	H7c (CH$_3$)	*2.0*	*11.7*	*3.40*

Intermolecular proximities are in italics.
[a] Distances are stated for the geometry-optimized (CASTEP) crystal structure.

Figure 2. Slices corresponding to a ^{1}H DQ frequency of 19.0 ppm, as extracted from 2-dimensional ^{1}H (850 MHz) DQ MAS (30 kHz) spectra of (a) the anhydrous HCl salt of cimetidine, (b) polymorph A of cimetidine, and (c-f) physical mixtures of polymorph A and the anhydrous HCl salt with (c) 10%, (d) 5%, (e) 1%, and (f) 0.5% w/w of polymorph A.

Table 4

Signal-to-Noise Ratios for the Peaks at a ^{1}H DQ Frequency of 19.0 ppm for the ^{1}H SQ H2 and H3 Resonances at 11.6 and 7.4 ppm (See Fig. 2) for Physical Mixtures of Polymorph A and the Anhydrous HCl Salt

w/w of Polymorph A (%)	H2	H3
10	16.6	16.2
5	6.3	7.0
1	3.3	2.4
0.5	1.6	1.0

polymorph A is observed in addition to the stronger ^{1}H DQ peaks at $\delta_{DQ} = 15.0 + 9.4 = 24.4$ ppm due to the anhydrous HCl salt. Thus, it is necessary to focus on the peaks observed at a ^{1}H DQ frequency of 19.0 ppm, and Figure 2 presents slices at this DQ frequency for (a) the anhydrous HCl salt of cimetidine, (b) polymorph A of cimetidine, and (c-f) physical mixtures of polymorph A with the anhydrous HCl salt with (c) 10%, (d) 5%, (e) 1%, and (f) 0.5% w/w of polymorph A. For the anhydrous HCl salt, we note that there are ^{1}H DQ peaks at $\delta_{DQ} = 15.0 + 4.0 = 19.0$ ppm due to proximity with aliphatic protons—see Figs. 1a and 2a. The spreading into 2 dimensions allows these to be distinguished from the ^{1}H DQ peaks at $\delta_{DQ} = 11.6 + 7.4 = 19.0$ ppm, characteristic of polymorph A. Following the dashed lines through the peaks at $\delta_{SQ} = 11.6$ and 7.4 ppm, it is observed that the ^{1}H DQ peaks due to polymorph A are still evident above the noise level down to the 1% w/w mixture in Figure 2e. This conclusion is confirmed by the signal-to-noise analysis presented in Table 4 for the peaks at a ^{1}H DQ frequency of 19.0 ppm for the H2 and H3 ^{1}H SQ resonances at 11.6 and 7.4 ppm. Following the guidance of the International Conference on Harmonisation of Technical Requirements for Registration of Pharmaceuticals for Human Use, Validation of Analytical Procedures: Text and Methodology Q2(R1), section 6.2 states that "A signal-to-noise ratio between 3 or 2:1 is generally considered acceptable for estimating the detection limit."[66] As such, the data in Table 4 establish 1% w/w as the level of detection using ^{1}H DQ MAS NMR at 30-kHz MAS and a ^{1}H Larmor frequency of 850 MHz for 2 crystalline phases of cimetidine.

Conclusions

Two distinct crystalline phases of cimetidine, polymorph A and the anhydrous HCl salt, are clearly distinguished using ^{1}H DQ MAS solid-state NMR spectroscopy by focusing on the pair of ^{1}H DQ peaks due to the intramolecular proximity (2.55 or 2.57 Å) of the neighboring H2 (CH) and H3 (NH) protons of the imidazole ring. Protonation at the N1 site in the anhydrous HCl salt as well as the fact that the 2 distinct solid-state forms have different intermolecular hydrogen-bonding arrangements leads to ^{1}H DQ peaks at $\delta_{DQ} = 15.0 + 9.4 = 24.4$ ppm for the anhydrous HCl salt and at $\delta_{DQ} = 11.6 + 7.4 = 19.0$ ppm for polymorph A. By spreading out the peaks into 2 dimensions, the observation of ^{1}H DQ peaks at $\delta_{DQ} = 11.6 + 7.4 = 19.0$ ppm is an unambiguous indicator of the presence of polymorph A. Using this "fingerprint", solid-state NMR experiments carried out at a ^{1}H Larmor frequency of 850 MHz and an MAS frequency of 30 kHz have shown that polymorph A can be detected and quantified in a physical mixture with the anhydrous HCl salt down to a concentration of 1% w/w. Considering literature reports (see Introduction), this level of detection matches and in some cases improves upon that reported for other analytical techniques, for example, PXRD, DSC, Raman spectroscopy, and THz spectroscopy. In particular, we emphasize that distinguishing between 2 crystalline phases represents a different challenge to the identification of a minority amount of a crystalline phase in the presence of an amorphous phase.

We note that employing ^{1}H DQ MAS represents a complementary approach to solid-state NMR of other nuclei, notably ^{13}C and ^{19}F.[67,68] Moreover, it has recently been shown that the sensitivity of solid-state NMR spectroscopy of moderately sized organic molecules can be significantly enhanced (e.g., by 5 times for paracetamol) by employing dynamic nuclear polarization, such that ^{13}C refocused INADEQUATE spectra can be recorded at natural isotopic abundance in 16 h for sulfathiazole (which has a long T_1 relaxation time, necessitating a recycle delay of 30 s)[69] and ^{15}N-^{1}H correlation spectra can be obtained also at natural isotopic abundance for a pharmaceutical formulation.[70] With the recent development of new dynamic nuclear polarization 1.3-mm MAS probe technology that allows faster MAS,[71] this approach seems promising for progressing to even lower levels of detection of minority solid-state forms by ^{1}H DQ MAS. This approach would also reduce the required experimental time (in this work, 19 h for the 2-dimensional spectrum of the 1% w/w sample), noting that experimental times are typically shorter for other techniques such as PXRD, Raman, and IR. Finally, as shown in our earlier work employing a ^{1}H DQ CRAMPS approach,[19] we note that the ^{1}H DQ solid-state NMR method presented here is readily applicable to tablet formulations with the shift of ^{1}H DQ peaks due to hydrogen-bonded protons to high ppm helping to avoid overlap with ^{1}H resonances of the excipients.

Acknowledgments

References

1. Serajuddin ATM. Salt formation to improve drug solubility. *Adv Drug Deliv Rev*. 2007;59:603-616.
2. Qu H, Savolainen M, Christensen LP, Rantanen J. Process-induced phase transformations in a pharmaceutically relevant salt-free form system. *Chem Eng Sci*. 2012;77:65-70.
3. Brittain HG. *Polymorphism in Pharmaceutical Solids*. 2nd ed. New York: Informa Healthcare; 2009.
4. Suda M, Takayama K, Otsuka M. An accurate quantitative analysis of polymorphic content by chemometric X-ray powder diffraction. *Anal Sci*. 2008;24:451-457.
5. Li Y, Chow PS, Tan RBH. Quantification of polymorphic impurity in an enantiotropic polymorph system using differential scanning calorimetry, X-ray powder diffraction and Raman spectroscopy. *Int J Pharm*. 2011;415:110-118.
6. Siddiqui A, Rahman Z, Bykadi S, Khan MA. Chemometric methods for the quantification of crystalline tacrolimus in solid dispersion by powder X-ray diffractrometry. *J Pharm Sci*. 2014;103:2819-2828.
7. Rahman Z, Bykadi S, Siddiqui A, Khan MA. Comparison of X-ray powder diffraction and solid-state nuclear magnetic resonance in estimating crystalline fraction of tacrolimus in sustained-release amorphous solid dispersion and development of discriminating dissolution method. *J Pharm Sci*. 2015;104:1777-1786.
8. Macfhionnghaile P, Hu Y, Gniado K, Curran S, McArdle P, Erxleben A. Effects of ball-milling and cryomilling on sulfamerazine polymorphs: a quantitative study. *J Pharm Sci*. 2014;103:1766-1778.
9. Zeitler JA, Taday PF, Newnham DA, Pepper M, Gordon KC, Rades T. Terahertz pulsed spectroscopy and imaging in the pharmaceutical setting - a review. *J Pharm Pharmacol*. 2007;59:209-223.
10. Strachan CJ, Taday PF, Newnham DA, et al. Using terahertz pulsed spectroscopy to quantify pharmaceutical polymorphism and crystallinity. *J Pharm Sci*. 2005;94:837-846.
11. Hisazumi J, Suzuki T, Nakagami H, Terada K. Quantification of pharmaceutical polymorphs and prediction of dissolution rate using theophylline tablet by terahertz spectroscopy. *Chem Pharm Bull*. 2011;59:442-446.
12. Thakral NK, Behme RJ, Aburub A, et al. Salt disproportionation in the solid state: role of solubility and counterion volatility. *Mol Pharm*. 2016;13:4141-4151.
13. Harris RK. NMR studies of organic polymorphs and solvates. *Analyst*. 2006;131:351-373.

14. Berendt RT, Sperger DM, Isbester PK, Munson EJ. Solid-state NMR spectroscopy in pharmaceutical research and analysis. *Trends Anal Chem*. 2006;25:977-984.

15. Harris RK. Applications of solid-state NMR to pharmaceutical polymorphism and related matters. *J Pharm Pharmacol*. 2007;59:225-239.

16. Geppi M, Mollica G, Borsacchi S, Veracini CA. Solid-state NMR studies of pharmaceutical systems. *Appl Spectros Rev*. 2008;43:202-302.

17. Vogt FG. Evolution of solid-state NMR in pharmaceutical analysis. *Future Med Chem*. 2010;2:915-921.

18. Mifsud N, Elena B, Pickard CJ, Lesage A, Emsley L. Assigning powders to crystal structures by high-resolution ^{1}H-^{1}H double quantum and ^{1}H-^{13}C J-INEPT solid-state NMR spectroscopy and first principles computation. A case study of penicillin G. *Phys Chem Chem Phys*. 2006;8:3418-3422.

19. Griffin JM, Martin DR, Brown SP. Distinguishing anhydrous and hydrous forms of an active pharmaceutical ingredient in a tablet formulation using solid-state NMR spectroscopy. *Angew Chem Int Ed Engl*. 2007;46:8036-8038.

20. Harris RK, Cadars S, Emsley L, et al. NMR crystallography of oxybuprocaine hydrochloride, modification II degrees. *Phys Chem Chem Phys*. 2007;9:360-368.

21. Zhou DH, Rienstra CM. Rapid analysis of organic compounds by proton-detected heteronuclear correlation NMR spectroscopy with 40 kHz magic-angle spinning. *Angew Chem Int Ed Engl*. 2008;47:7328-7331.

22. Salager E, Stein RS, Pickard CJ, Elena B, Emsley L. Powder NMR crystallography of thymol. *Phys Chem Chem Phys*. 2009;11:2610-2621.

23. Vogt FG, Clawson JS, Strohmeier M, Edwards AJ, Pham TN, Watson SA. Solid-state NMR analysis of organic cocrystals and complexes. *Cryst Growth Des*. 2009;9:921-937.

24. Guilbaud JB, Clark BC, Meehan E, Hughes L, Saiani A, Khimyak YZ. Effect of encapsulating a pseudo-decapeptide containing arginine on PLGA: a solid-state NMR study. *J Pharm Sci*. 2010;99:2681-2696.

25. Khan M, Enkelmann V, Brunklaus G. Crystal engineering of pharmaceutical co-crystals: application of methyl paraben as molecular hook. *J Am Chem Soc*. 2010;132:5254-5263.

26. Pham TN, Watson SA, Edwards AJ, et al. Analysis of amorphous solid dispersions using 2D solid-state NMR and ^{1}H T_1 relaxation measurements. *Mol Pharm*. 2010;7:1667-1691.

27. Bettini R, Menabeni R, Tozzi R, et al. Didanosine polymorphism in a super-critical antisolvent process. *J Pharm Sci*. 2010;99:1855-1870.

28. Harris RK, Hodgkinson P, Zorin V, et al. Computation and NMR crystallography of terbutaline sulfate. *Magn Reson Chem*. 2010;48:S103-S112.

29. Khan MKM, Enkelmann V, Brunklaus G. Heterosynthon mediated tailored synthesis of pharmaceutical complexes: a solid-state NMR approach. *CrystEngComm*. 2011;13:3213-3223.

30. Bradley JP, Velaga SP, Antzutkin ON, Brown SP. Probing intermolecular crystal packing in γ-indomethacin by high-resolution ^{1}H solid-state NMR spectroscopy. *Cryst Growth Des*. 2011;11:3463-3471.

31. Mafra L, Santos SM, Siegel R, et al. Packing interactions in hydrated and anhydrous forms of the antibiotic ciprofloxacin: a solid-state NMR, X-ray diffraction, and computer simulation study. *J Am Chem Soc*. 2012;134:71-74.

32. Bradley JP, Pickard CJ, Burley JC, et al. Probing intermolecular hydrogen bonding in sibenadet hydrochloride polymorphs by high-resolution ^{1}H double-quantum solid-state NMR spectroscopy. *J Pharm Sci*. 2012;101:1821-1830.

33. Tatton AS, Pham TN, Vogt FG, Iuga D, Edwards AJ, Brown SP. Probing intermolecular interactions and nitrogen protonation in pharmaceuticals by novel ^{15}N-edited and 2D ^{14}N-^{1}H solid-state NMR. *CrystEngComm*. 2012;14:2654-2659.

34. Maruyoshi K, Iuga D, Antzutkin ON, Alhalaweh A, Velaga SP, Brown SP. Identifying the intermolecular hydrogen-bonding supramolecular synthons in an indomethacin-nicotinamide cocrystal by solid-state NMR. *Chem Commun*. 2012;48:10844-10846.

35. Tatton AS, Pham TN, Vogt FG, Iuga D, Edwards AJ, Brown SP. Probing hydrogen bonding in cocrystals and amorphous dispersions using ^{14}N-^{1}H HMQC solid-state NMR. *Mol Pharm*. 2013;10:999-1007.

36. Baias M, Widdifield CM, Dumez JN, et al. Powder crystallography of pharmaceutical materials by combined crystal structure prediction and solid-state ^{1}H NMR spectroscopy. *Phys Chem Chem Phys*. 2013;15:8069-8080.

37. Carignani E, Borsacchi S, Bradley JP, Brown SP, Geppi M. Strong intermolecular ring current influence on ^{1}H chemical shifts in two crystalline forms of naproxen: a combined solid-state NMR and DFT study. *J Phys Chem C*. 2013;117:17731-17740.

38. Czernek J, Brus J. Theoretical predictions of the two-dimensional solid-state NMR spectra: a case study of the ^{13}C–^{1}H correlations in mergoline. *Chem Phys Lett*. 2013;586:56-60.

39. Baias M, Lesage A, Aguado S, et al. Superstructure of a substituted zeolitic imidazolate metal-organic framework determined by combining proton solid-state NMR spectroscopy and DFT calculations. *Angew Chem Int Ed Engl*. 2015;54:5971-5976.

40. Fernandes JA, Sardo M, Mafra L, Choquesillo-Lazarte D, Masciocchi N. X-ray and NMR crystallography studies of novel theophylline cocrystals prepared by liquid assisted grinding. *Cryst Growth Des*. 2015;15:3674-3683.

41. Xu J, Terskikh VV, Chu YY, Zheng AM, Huang YN. Mapping out chemically similar, crystallographically nonequivalent hydrogen sites in metal-organic frameworks by ^{1}H solid-state NMR spectroscopy. *Chem Mater*. 2015;27:3306-3316.

42. Krajnc A, Kos T, Logar NZ, Mali G. A simple NMR-based method for studying the spatial distribution of linkers within mixed-linker metal-organic frameworks. *Angew Chem Int Ed Engl*. 2015;54:10535-10538.

43. Luedeker D, Gossmann R, Langer K, Brunklaus G. Crystal engineering of pharmaceutical co-crystals: "NMR crystallography" of niclosamide co-crystals. *Cryst Growth Des*. 2016;16:3087-3100.

44. Brunklaus G, Koller H, Zones SI. Defect models of as-made high-silica zeolites: clusters of hydrogen-bonds and their interaction with the organic structure-directing agents determined from ^{1}H double and triple quantum NMR spectroscopy. *Angew Chem Int Ed Engl*. 2016;55:14457-14461.

45. Dudek MK, Jeziorna A, Potrzebowski MJ. Computational and experimental study of reversible hydration/dehydration processes in molecular crystals of natural products - a case of catechin. *CrystEngComm*. 2016;18:5267-5277.

46. Dudek MK, Pawlak T, Paluch P, Jeziorna A, Potrzebowski MJ. A multi-technique experimental and computational approach to study the dehydration processes in the crystals of endomorphin opioid peptide derivative. *Cryst Growth Des*. 2016;16:5312-5322.

47. Abraham A, Apperley DC, Byard SJ, et al. Characterising the role of water in sildenafil citrate by NMR crystallography. *CrystEngComm*. 2016;18:1054-1063.

48. Widdifield CM, Robson H, Hodgkinson P. Furosemide's one little hydrogen atom: NMR crystallography structure verification of powdered molecular organics. *Chem Commun*. 2016;52:6685-6688.

49. Brown SP. Probing proton-proton proximities in the solid state. *Prog Nucl Magn Reson Spectrosc*. 2007;50:199-251.

50. Brown SP. Recent advances in solid-state MAS NMR methodology for probing structure and dynamics in polymeric and supramolecular systems. *Macromol Rapid Commun*. 2009;30:688-716.

51. Brown SP. Applications of high-resolution ^{1}H solid-state NMR. *Solid State Nucl Magn Reson*. 2012;41:1-27.

52. Brown SP, Lesage A, Elena B, Emsley L. Probing proton-proton proximities in the solid state: high-resolution two-dimensional ^{1}H-^{1}H double-quantum CRAMPS NMR spectroscopy. *J Am Chem Soc*. 2004;126:13230-13231.

53. Watts AE, Maruyoshi K, Hughes CE, Brown SP, Harris KDM. Combining the advantages of powder X-ray diffraction and NMR crystallography in structure determination of the pharmaceutical material cimetidine hydrochloride. *Cryst Growth Des*. 2016;16:1798-1804.

54. Sommer W, Gottwald J, Demco DE, Spiess HW. Dipolar heteronuclear multiple-quantum NMR-spectroscopy in rotating solids. *J Magn Reson*. 1995;113:131-134.

55. Schnell I, Lupulescu A, Hafner S, Demco DE, Spiess HW. Resolution enhancement in multiple-quantum MAS NMR spectroscopy. *J Magn Reson*. 1998;133:61-69.

56. Brown SP, Spiess HW. Advanced solid-state NMR methods for the elucidation of structure and dynamics of molecular, macromolecular, and supramolecular systems. *Chem Rev*. 2001;101:4125-4155.

57. Hayashi S, Hayamizu K. Chemical shift standards in high-resolution solid-state NMR (1) ^{13}C, ^{29}Si, and ^{1}H nuclei. *Bull Chem Soc Jpn*. 1991;64:685-687.

58. Middleton DA, Peng X, Saunders D, Shankland K, David WIF, Markvardsen AJ. Conformational analysis by solid-state NMR and its application to restrained structure determination from powder diffraction data. *Chem Commun*. 2002;(17):1976-1977.

59. Madine J, Middleton DA. An NMR strategy for obtaining multiple conformational constraints for ^{15}N-^{13}C spin-pair labelled organic solids. *Phys Chem Chem Phys*. 2006;8:5223-5228.

60. Pickard CJ, Mauri F. All-electron magnetic response with pseudopotentials: NMR chemical shifts. *Phys Rev B*. 2001;63:245101.

61. Yates JR, Pickard CJ, Mauri F. Calculation of NMR chemical shifts for extended systems using ultrasoft pseudopotentials. *Phys Rev B*. 2007;76:024401.

62. Hadicke E, Frickel F, Franke A. Die Struktur von Cimetidin (N″-cyan-N-methyl-N′-[2-[(5-methyl-1H-imidazol-4-yl)methylthio]ethyl]guanidin), einem histamin H$_2$-receptor-antagonist. *Chem Ber*. 1978;111:3222-3232.

63. Samoson A, Tuherm T, Gan Z. High-field high-speed MAS resolution enhancement in ^{1}H NMR spectroscopy of solids. *Solid State Nucl Magn Reson*. 2001;20:130-136.

64. Zorin VE, Brown SP, Hodgkinson P. Origins of linewidth in ^{1}H magic-angle spinning NMR. *J Chem Phys*. 2006;125:144508.

65. Bradley JP, Tripon C, Filip C, Brown SP. Determining relative proton-proton proximities from the build-up of two-dimensional correlation peaks in ^{1}H double-quantum MAS NMR: insight from multi-spin density-matrix simulations. *Phys Chem Chem Phys*. 2009;11:6941-6952.

66. International Conference on Harmonization. International Conference on Harmonization of Technical Requirements for Registration of Pharmaceuticals for Human Use. ICH Harmonised Tripartite Guideline Validation of Analytical Procedures: Text and Methodology; Q2(R1); Current Step 4 version. Geneva, Switzerland: ICH; 1994. Available at: http://www.ich.org/fileadmin/Public_Web_Site/ICH_Products/Guidelines/Quality/Q2_R1/Step4/Q2_R1__Guideline.pdf. Accessed July 5, 2017.

67. Virtanen T, Maunu SL. Quantitation of a polymorphic mixture of an active pharmaceutical ingredient with solid state ^{13}C CPMAS NMR spectroscopy. *Int J Pharm*. 2010;394:18-25.

68. Barry SJ, Pham TN, Borman PJ, Edwards AJ, Watson SA. A risk-based statistical investigation of the quantification of polymorphic purity of a pharmaceutical candidate by solid-state ^{19}F NMR. *Anal Chim Acta*. 2012;712:30-36.

69. Rossini AJ, Zagdoun A, Hegner F, et al. Dynamic nuclear polarization NMR spectroscopy of microcrystalline solids. *J Am Chem Soc*. 2012;134:16899-16908.

70. Rossini AJ, Widdifield CM, Zagdoun A, et al. Dynamic nuclear polarization enhanced NMR spectroscopy for pharmaceutical formulations. *J Am Chem Soc*. 2014;136:2324-2334.

71. Chaudhari SR, Berruyer P, Gajan D, et al. Dynamic nuclear polarization at 40 kHz magic angle spinning. *Phys Chem Chem Phys*. 2016;18:10616-10622.

72. Maruyoshi K, Iuga D, Brown SP. What is the lowest concentration of a minor free from component than can be detected by ^{1}H DQ MAS experiments in pharmaceutical solids? *Bull Magn Reson Soc Jpn*. 2014;5:76-77.